



6th BSME International Conference on Thermal Engineering (ICTE 2014)

## Characteristics of transient heat transfer and wetting phenomena during laminar jet quenching on rotating cylinder

Shinya Tsuboyama<sup>a</sup>, <sup>a</sup>Tomofumi Higashi<sup>a</sup>, Yuichi Mitsutake<sup>b\*</sup>, Suhaimi bin Illias<sup>a</sup>, Aloke Kumar Mazumder<sup>c</sup>, Koutaro Tsubaki<sup>a</sup> and Masanori Monde<sup>d</sup>

<sup>a</sup>Graduate school of Science and Technology, Saga University, 1 Honjo-machi, Saga-shi, Saga 840-8502, Japan

<sup>b</sup>Institute of Ocean Energy, Saga University, 1 Honjo-machi, Saga-shi, Saga 840-8502, Japan

<sup>c</sup>Department of Mechanical Engineering, Bangladesh University of Engineering & Technology, Dhaka 1000, Bangladesh

<sup>d</sup>International Research Center for Hydrogen Energy, Kyushu University, 744 Motoooka, Nishi-ku, Fukuoka-shi, Fukuoka, 819-0935, Japan

### Abstract

Hot strip leaving from finishing roll is quenched from about 850 to 500 °C by array of laminar jets on cooling table (Run-Out-Table). Cooling temperature control of the hot strip is important to obtain better mechanical strength and grain size. However, the cooling process includes unstable transition boiling region as well as moving boundary problem due to relative movement between the hot strip and the jets. To improve quality of hot strip deeper understanding about laminar jet quenching process on the moving hot surface should be elucidated. In this study, single laminar jet quenching tests on a rotating hollow hot cylinder mounted horizontally have been conducted to understand characteristics of transient heat transfer and wetting phenomena. The experiments were done for 18-8 stainless steel (SUS304) hollow cylinder (O.D. 136mm, I.D. 116mm, W 150mm) under rotational speed ranged from 15 to 60 rpm, cooling water temperature ranged from 10 to 60 °C (corresponding degree of subcooling 40-90 K) and flow rate ranged from 6 to 23 L/min. Surface temperature and surface heat flux on the rotating cylinder were estimated from two sheath thermocouples embedded at two depths from the outer surface with one dimensional inverse heat conduction analysis. Visual observations over the top surface were done with two normal speed video cameras which were synchronized with rotating cylinder temperature recording. The observation results showed that unstable wetted area was gradually growing from the stagnation area and finally the wetted area became continuous around the circumference of the cylinder. It was found that the growth and shape of the wetted area were strongly affected by the liquid temperature and the liquid flow rate. Wetted front which is the boundary between wetted and dry areas repeated advance and recession. Since the wetting area propagated faster in the rotational direction, the shape of the wetted area was asymmetry on the hot surface. The liquid film flow was completely splashed out due to violent nucleate boiling on the wetted front line. The characteristics of local transient heat transfer were evaluated with boiling curves taken around the stagnation point. The boiling curves indicated shift to much

\* Corresponding author. Tel.: +81-952-28-8616; fax: +81-952-28-8587.

E-mail address: [mitsutake@me.saga-u.ac.jp](mailto:mitsutake@me.saga-u.ac.jp)

higher wall superheat as compared with a steady state pool boiling curve and those were categorized into three regions such as 1) single phase heat transfer, boiling heat transfer and 3) transition boiling by inspecting gradient of the boiling curves and the observation of the boiling situations. The transition boiling region disappeared and the single phase heat transfer became dominant for higher subcooling and higher flow rate conditions.

© 2015 The Authors. Published by Elsevier Ltd. This is an open access article under the CC BY-NC-ND license (<http://creativecommons.org/licenses/by-nc-nd/4.0/>).

Peer-review under responsibility of organizing committee of the 6th BSME International Conference on Thermal Engineering (ICTE 2014)

**Keywords:** Lamellar jet; Transient transition boiling; Wetting phenomenon; Quenching

## 1. Introduction

Steel manufacturing industries are trying to improve thermomechanical treatment processes to produce high value added hot strips such as high tensile stress (HTS), dual phase (DP) and transformation induced plasticity (TRIP) steels. In order to reduce adding expensive minor metal elements like nickel or manganese to carbon steel, precise temperature control of low alloy hot strips over entire of width and length attracts great interest to produce such high value added steels. In case of the TRIP steel production process, the hot strip at about 800°C is quenched to about 400 °C with laminar or spray jets impingement on run-out-table (ROT) after finishing roll. To ensure mechanical properties, a severe allowance error of terminate cooling temperature is required for controlled cooling of the strip. Even though state of art control technology such as learning or predictive control is applied to online control of hot strip temperature at the exit of the ROT, accuracy of temperature control and process yield still do not reach to a satisfactory level. Especially when the terminate strip temperature is in the transition boiling region empirically known as 500-550 °C in steel manufacturing industries, control of the hot strip temperature becomes difficult due to the unstable transition boiling heat transfer. In the transition boiling, boiling situation changes from film boiling to nucleate boiling due to recovery of wetting on hot surface. Since the surface heat transfer coefficient dramatically changes whether the surface is wetted or not, the temperature control faces with difficulties of the unstable boiling heat transfer. Rewetting phenomenon is also known to be very sensible to surface conditions such as surface roughness, thickness of poor heat conductive oxidation layer as well as coolant conditions as water temperature and intensity of liquid impact pressure on a hot surface. Despite of many studies and challenges to understand the transient transition boiling heat transfer and the wetting process on hot surface, a lot of elementary processes about this phenomenon are still remained for us.

Recently considerable studies on quenching hot surface at high initial temperature up to 800-900 °C with pipe laminar, slit laminar and flat spray jets were reported and characteristics of transient transition boiling heat transfer were reported to understand fundamental boiling process from film to transition boilings. However, thin strip of a couple of millimeters in thickness is quenched during transfer on ROT at maximum velocity of 60 km/h. Thus quenching process of the strips becomes moving heat sink boundary problem. However, reproduce of similar experiments with real processes are very difficult in a laboratory. Most of existing experimental studies were done for stationary heated surface and experiments with moving surface are limited as far as the authors know.

For example, Gradeck, et al. [1] conducted experimental study on boiling heat transfer during quenching of rotating hot hollow cylinder with a slit laminar jet. Quenching heat transfer distributions were obtained for different rotational speed by using boiling curves. Alope, et al. [2] also reported experimental study on laminar jet quenching on rotating hollow cylinder as our previous study. Characteristics of non-uniform wetting front propagation which was identified as the location at leading edge of the wetted area, and comparison of maximum heat flux with steady state critical heat flux were elucidated at two rotational speeds and different flow rates and coolant water temperatures.

In this study we conducted experiments using the previous experimental apparatus [2] over the extensive experimental range of coolant water temperature, laminar flow rate and rotational speed. Image analysis of boiling situation video provided the characteristic of rewetting process on the moving hot surface. Surface temperature and surface heat flux on the outer surface were evaluated with one dimensional inverse heat conduction analysis. Effects

of circumferential position, coolant water temperature, laminar flow rate and rotational speed on boiling curve were elucidated in particular.

### Nomenclature

$a$	thermal diffusivity ( $\text{m}^2/\text{s}$ )
$d_j$	inner diameter of the laminar jet nozzle (m)
$N$	rotational speed of cylinder (rpm)
$q_w$	surface heat flux ( $\text{W}/\text{m}^2$ )
$Q$	volumetric flow rate of laminar jet (L/min)
$r$	radial coordinate (mm)
$S$	circumferential coordinate of curvilinear coordinates system on the outer surface of the cylinder (mm)
$t$	time (s)
$t_{wet,i}$	time when the stable wetting area was formed at the stagnation point (s)
$t_{wet,f}$	time when the circumferentially continuous wetting area was formed around the cylinder (s)
$T_b$	measured temperature in the cylinder wall ( $^{\circ}\text{C}$ )
$T_{bo}$	initial temperature of the cylinder ( $^{\circ}\text{C}$ )
$T_l$	laminar water jet temperature ( $^{\circ}\text{C}$ )
$T_w$	surface temperature ( $^{\circ}\text{C}$ )
$W_s$	characteristic dimension of wetting front distribution in circumferential direction (mm) (See Fig.4(b))
$W_x$	characteristic dimension of wetting front distribution in axial direction (mm) (See Fig.4(b))
$X$	axial coordinate of curvilinear coordinates system on outer surface of the cylinder (mm)
$y$	depth from the outer surface (mm)
$z$	axial coordinate (mm)
Greek letters	
$\Delta T_{sat}$	wall superheat (K)
$\Delta T_{sub}$	degree of liquid subcooling (K)
$\lambda$	thermal conductivity ( $\text{W}/\text{m}/\text{K}$ )
$\theta$	angular position of thermocouple (rad)

## 2. Experimental apparatus and procedure

### 2.1. Experimental apparatus

The schematic of the experimental apparatus is shown in Fig.1. A rotating hollow cylinder mounted horizontally was quenched by a downward single laminar water jet. The water supply system circulated water between the bottom and upper tanks of total capacity 350 L with a feed water pump and controlled water temperature at designated temperature up to  $60^{\circ}\text{C}$  with by total 16 kW heater equipped with the tanks. The water was supplied to the nozzle at a constant water head from the upper overhead tank. The laminar jet velocity was evaluated with pressure loss between the inlet and outlet of the nozzle and the flow coefficient of the nozzle calibrated by preliminary test. The test cylinder was rotated in anti-clockwise as indicated arrows in Fig.1. Two cameras took movie of wetting surface. The top of 202.2 degree of the cylinder surface was observed with the cameras. Start time of recording with the cameras was synchronized with the data acquisition system.

Figure 2 shows the dimension of the tested hollow cylinder and locations of thermocouples embedded in the cylinder wall. The test cylinder was 150 mm in length, 136 mm in outer diameter and 116 mm in inner diameter. The test cylinder material was SUS304 which has no phase transition point over the experimental temperature range from  $10^{\circ}\text{C}$  to  $900^{\circ}\text{C}$ . The grounded K-type sheath thermocouples of O.D. 1 mm were embedded at the axial center position at the two different depths of 1.5 and 3.5 mm from the outer surface. Two different radially located thermocouples were directed to the angular directions of  $\theta = 0$  and  $\pi$  as shown in Fig.2. Surface temperature and surface heat flux were evaluated with the one-dimensional transient inverse heat conduction analysis proposed by

the authors [3] from measured temperature histories. The hollow cylinder was heated to initial temperature in an electric furnace and then it was mounted horizontally on the test bench as shown in Fig.3. The test cylinder was rotated with a pulse motor drive unit at a designated rotational speed. Thermoelectromotive force signals from the thermocouples were transmitted to an instrumental apparatus via 8ch mercury rotary contactors. The test bench was mounted on the bottom tank so that the axially center point of the cylinder was adjusted to the stagnation point of the laminar jet.

## 2.2. Experimental condition and procedure

The present experiments have been done by changing in the rotational speed  $N$ , the water temperature  $T_l$  (liquid subcooling  $\Delta T_{sub}$ ) and the laminar jet flow rate  $Q$  as the experimental parameters. The range of these parameters is tabulated in Table 1. The rotational speed of the cylinder was decided by the similarity of the thick hollow cylinder wall with thin hot strip. For example, ratio of Fourier numbers at a certain time for 1 mm of low carbon steel wall ( $\alpha = 1.4 \times 10^{-5} \text{ m}^2/\text{s}$ ) and 10 mm of stainless steel SUS304 wall ( $\alpha = 4.01 \times 10^{-6} \text{ m}^2/\text{s}$ ) becomes about 350. That means that the stainless temperature changes at about 350 times slower than that of the low carbon steel. Therefore, circumferential velocity of the stainless steel hollow cylinder at  $N = 15 \text{ rpm}$  corresponds to the equivalent moving velocity of 67 km/h for the low carbon steel. A large time scale factor between the tested hollow cylinder and thin strip brings advantages to designing the experimental apparatus and making measurement of transient temperature in the wall easier in laboratory tests. Thus we selected the rotational speeds from 15 to 60 rpm which corresponds to the real hot strip transfer velocity.

The storage water was heated at experimental liquid subcooling during water circulation between the tanks. During heating feed water, opening of the flow control valve was previously adjusted to the designated liquid flow rate. To prevent the laminar water jet from impinging on the hot test cylinder before starting experiment, water supply to the laminar nozzle was bypassed to the bottom tank through the three-side cock.

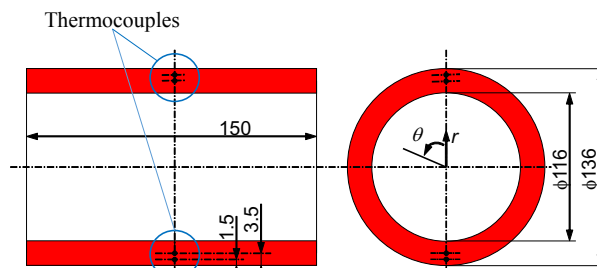
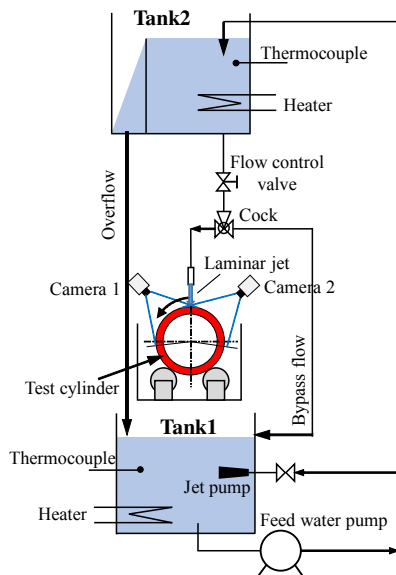


Fig.2 Dimension of the test cylinder and locations of thermocouples

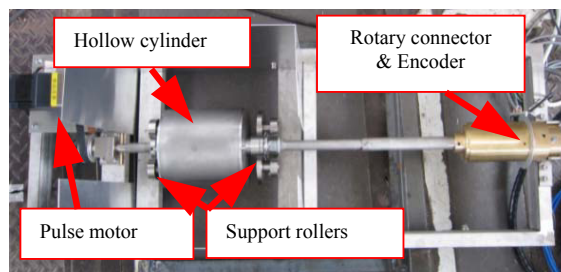


Fig.1 Experimental apparatus (water circulation system) Fig.3 Top view of the test bench

Table 1 Experimental range.

Inner diameter of laminar nozzle $d_i$ [mm]	15
Subcooling of Water $\Delta T_{sub}$ [K]	50, 60, 70, 80, 90
Flow rate of laminar jet $Q$ [L/min]	6, 10, 15, 23

Impinging jet velocity $u_j$ [m/s]	1.3, 1.6, 2.0, 2.8
Initial temperature of cylinder $T_{bo}$ [°C]	780 – 805
Rotational speed of cylinder $N$ [rpm]	15, 20, 30, 60
circumferential speed of outer cylinder surface $v_\theta$ [m/s]	0.11, 0.14, 0.21, 0.42

The test cylinder suspended in a crucible electric furnace was heated to up to 870 °C. Then, the test cylinder was got out and mounted on the test bench and then transferred just beneath the laminar jet nozzle as soon as possible. The pulse motor drive system was switched on and the data acquisition system and the two video cameras (30 fps) were triggered to start recording by the rotary encoder. The trigger signal was synchronized with the rotational angle of the thermocouples precisely. Then the three-side cock was turned to start laminar jet quenching. The video cameras recorded change in boiling situation on the upper half of the rotating cylinder surface. The laminar jet impingement ceased until wetted area continuously covered around the circumference of the cylinder surface.

### 3. Experimental results and discussion

#### 3.1. Visual observation of boiling situation during quenching of rotation hollow cylinder

Typical boiling situation on the rotating cylinder at elapsed time of 14 s after starting laminar jet quenching was shown in Fig. 4. The corresponding experimental condition was for the rotational speed of  $N = 60$  rpm, the liquid subcooling of  $\Delta T_{sub} = 70$  K and the flow rate of  $Q = 10$  L/min. The rotational direction of the test cylinder was denoted with the yellow arrow. Stagnation point of the laminar jet on the hot surface was indicated with the white dot and the arrow. A black area distributing around the stagnation point was covered with single phase liquid film (S.P.F.) and steady liquid-solid contact and single phase convective heat transfer were observed but net bubble nucleation was invisible. The outer boundary of S.P.F. denoted with the blue dashed line agreed with the onset of nucleate boiling (O.N.B.) locations beyond which violent nucleate boiling (N.B.) took place. The nucleate boiling region was visible as bright (white) zone in the photo, and the region size was ranged from a few millimeters to tens of millimeters depending on the direction from the stagnation point. On the downstream of the S.P.F. area just behind the O.N.B., subcooled boiling (S.B.) area accompanied weak surface boiling was also observed. The liquid film flow along the surface was completely splashed out as droplets at the outer edge of the N.B. region and the hot surface was dry on the hot surface outside of the N.B. region. The boundary between the dry and the nucleate boiling regions, namely the leading edge of the wetting area denoted as the wetting front (W.F.) and it specifies wetted area on which the major cooling heat transfer occurs. Therefore, we have a great interest in growth of W.F. during laminar jet quenching and retrieved change in locus of W.F. with time by image processing of boiling videos. Figure 4(b) indicates distributions of the O.N.B. and the W.F. as the blue dashed and the red lines which were taken at elapsed time of 14 s under the same experimental condition of Fig. 4(a). The origin of Fig. 4(b) was taken at the stagnation point and the longitudinal and abscissa axes were taken as the circumferential direction of  $S$  and the axial direction of  $X$ , respectively. It is noted that the negative direction of  $S$  agrees with the rotational direction. Additionally characteristic dimensions of W.F. in the circumferential and axial directions were defined as  $W_s$  and  $W_x$  in Fig. 4 (b).

As shown in Figs. 4 (a) and (b), the loci of the O.N.B. and W.F. indicated asymmetry in the circumferential direction and expanded faster in the rotational direction as compared with the inverse rotational and axial directions. In case of jet quenching on a stationary hot surface [4], the loci of O.N.B. and W.F. indicated concentric circles which were symmetric with respect to the stagnation point.

#### 3.2. Change in characteristic dimensions of wetting front distribution $W_s$ , $W_x$ with time

Typical examples for changes in  $W_s$  and  $W_x$  of the W.F. distribution with time are shown in Figs. 5(a) and (b). The experimental condition was for  $N = 20$  rpm,  $\Delta T_{sub} = 70$  K and  $Q = 10$  L/min. The reference time of 0 s in the graphs was defined as the time when the reference thermocouple at  $\theta = 0$  deg passed first beneath the stagnation point just

after the jet quenching started. The definition of the reference time  $t = 0$  was commonly used in showing time histories of transient data given later.

In Fig. 5(a) the locations of the both ends of W.F. in circumference direction  $+W_s / -W_s$  were denoted as the red and blue lines, and the characteristic circumferential length of  $W_s$  as the black line. The locations of the both ends in axial direction  $+W_x / -W_x$  and the characteristic axial length  $W_x$  were also depicted in Fig. 5(b) in the similar way. It is found that propagation of the W.F. in the circumference direction was categorized into four time regimes denoted as (a)-(d). Each photo of boiling situation taken at corresponding regime from (a) to (d) was shown in Fig. 6(a)-(d), respectively. The regime (a) with no symbols referred as “non-wetted regime” at which the laminar jet hardly contacted with the hot surface even at the stagnation point and it separated as very smooth thin liquid film flow along the surface as shown in Fig. 6(a). The regime (b) referred as “unstable wetting regime” was started at about 4 s, and the location of  $-W_s$  in the rotational direction gradually increased first by repeating advance and recession. However, propagation of  $+W_s$  in the opposite direction was suppressed until 11 s. The W.F. was gradually advancing along the surface by repeating advance and recession. In the regime (c) after 20 s denoted as “uniform advancing rate regime”, surface wetting situation around the stagnation was stabilized and the wetting front monotonously and gradually advanced to the circumference direction with time. Finally the W.F. started advancing rapidly to form the circumferentially continuous wetted area around the cylinder in the regime (d) characterized with “rapid W.F. advancing regime”.

In contrast, constant moving velocity of the W.F. in the both axial directions of  $+X / -X$  was indicated during entire the regimes in Fig. 5(b). Moving velocity of W.F. in the axial direction indicated was smaller than that in the rotational direction.

### 3.3. Fluctuations of internal temperatures with time

Measured typical internal temperature history at each thermocouple position with time is shown in Fig. 7 (a) for the condition of  $N = 20$  rpm,  $T_l = 30$  °C,  $T_{bo} = 785$  °C and  $Q = 10$  L/min. The black and red solid lines show the temperature histories of  $\theta = 0$  and  $\pi$  at the depth of 1.5 mm from the outer surface. The blue and green dotted lines are given for  $\theta = 0$  and  $\pi$  at the depth of 3.5 mm. The symbols plotted on the lines at the interval of 3 s show the time when the

a

b

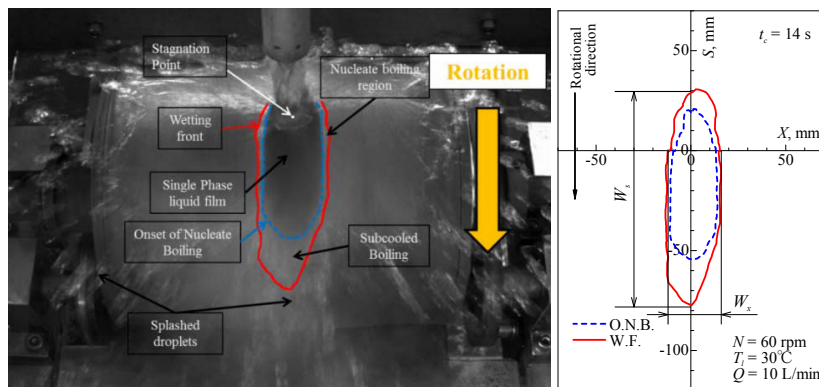


Fig. 4 Definitions of flow boiling heat transfer regions, onset of nucleate boiling (O.N.B.) and wetting front (W.F.) line on the rotating hot surface. (a) Photograph of boiling situation (b) shapes of O.N.B and W.F. lines evaluated by video image analysis

ab



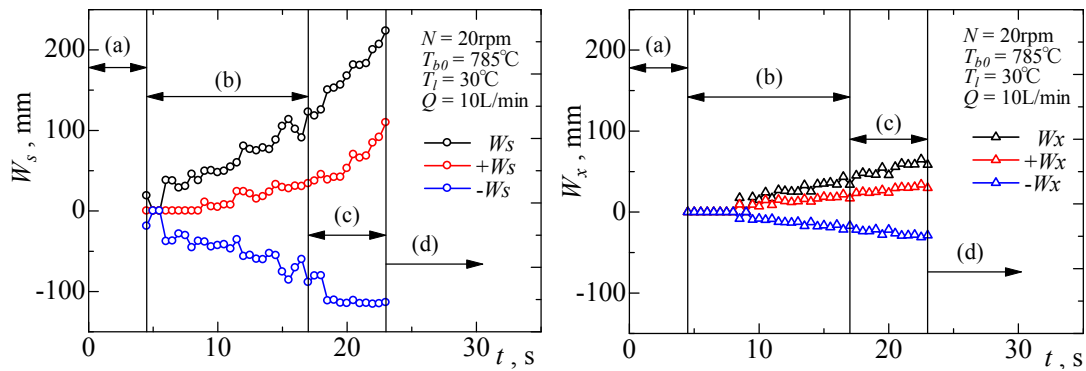


Fig.5 Change of characteristic dimensions of wetting area with time. (a) Circumferential length  $W_s$  (b) Axial length  $W_x$

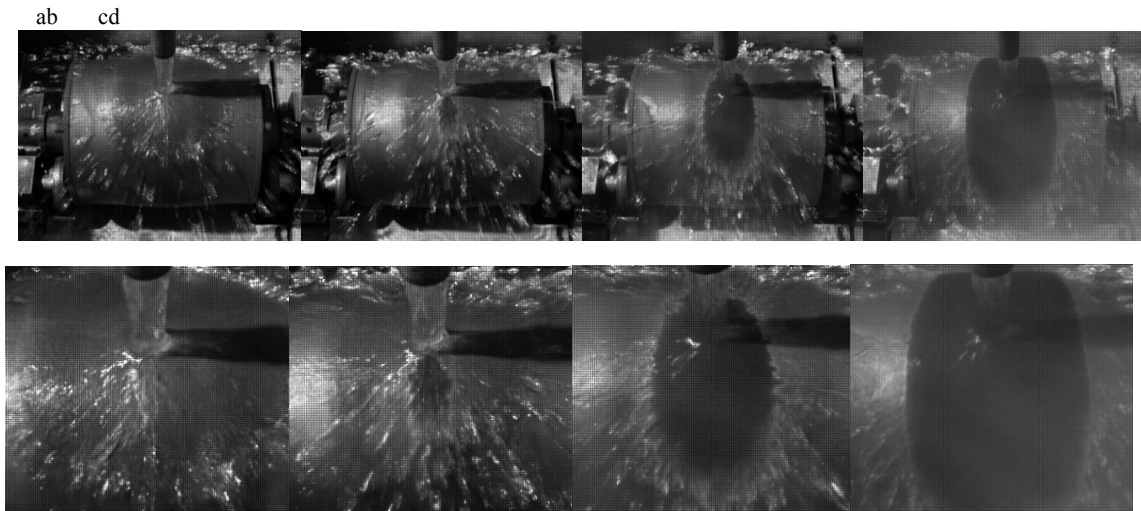


Fig.6 Photos of boiling situation on the rotor (upper side) and close-up of the stagnation area (lower side) during development of surface rewetting taken at the regimes (a) Non-wetted regime, (b) Unstable wetting regime, (c) Uniform and slow advance regime and (d) Rapid spread of wetting

thermocouple passed beneath the nozzle. The arrows denoted as  $t_{wet,i}$  and  $t_{wet,f}$  indicate the times when the stable wetted area was observed (inception time of the regime (b)) and the circumferentially continuous wetted area was achieved on the hot surface, respectively.

It is found that the measured temperatures fluctuated at the period of 3 s in synchronization with passing the stagnation point and the fluctuations at  $\theta = 0$  exactly advanced as half period of 1.5 s against the fluctuations at  $\theta = \pi$ . These results were caused by the cooling on the wetted surface around the stagnation point and the reheating on the dry area. Noting symbols on each temperature history, we can see sudden drops at the depth of 1.5 mm started just before the thermocouple arrived at the stagnation point. The wetted area spread around the stagnation point. Amplitude of the temperature fluctuation gradually increased and recorded maximum just after the inception of stable surface wetting denoted as  $t_{wet,i}$ . And then the amplitude decreased as repeating the cylinder rotations and disappeared after  $t_{wet,f}$  due to the continuous wetted situation around the cylinder. Meanwhile comparing temperature histories at  $y = 1.5$  mm and 3.5 mm, we can see that temperature fluctuation attenuated as the radial position became deeper from the outer surface as the result of the nature of the temperature wave propagation with conduction of heat in solid.

ab

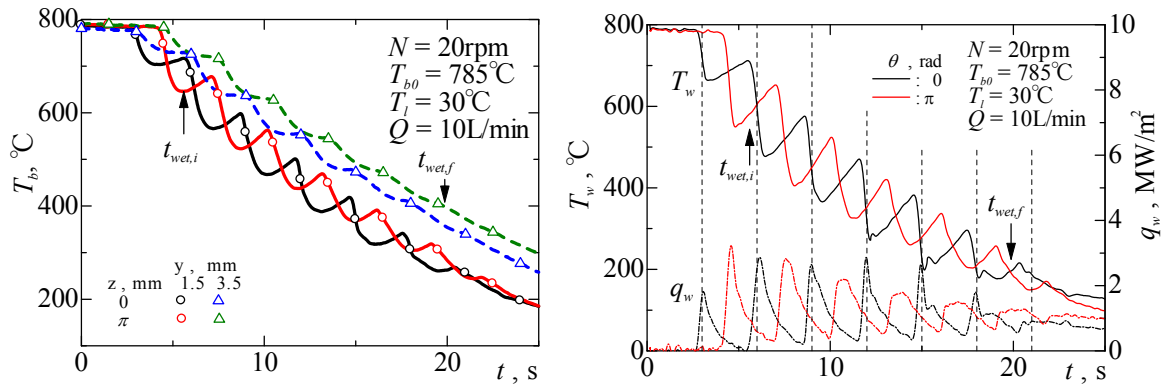


Fig.7 Measured temperature and heat flux with time for rotational speed  $N = 20 \text{ rpm}$ , laminar jet temperature  $T_l = 30^\circ\text{C}$  and laminar flow rate  $Q = 10 \text{ L/min}$ . (a) Temperature fluctuations during laminar jet cooling of rotating hollow cylinder, (b) Change in surface temperature and heat flux

### 3.4. Estimated surface temperature and surface heat flux with inverse heat conduction analysis

The surface temperature and surface heat flux were evaluated by the inverse program analysis technique [3] proposed by the authors. Discussions of the evaluated surface heat transfers will be given below. Typical change in surface temperature  $T_w$  and surface heat flux  $q_w$  with time is shown in Fig.7 (b). The vertical dashed lines indicate the times when the thermocouple position passed beneath the laminar nozzle. The  $T_w$  indicates very sharp drop in synchronization with passing stagnation point denoted with the dashed lines. Just after  $t_{wet,i}$  drop in  $T_w$  recorded the maximum value, and then cooling duration became longer and amplitude of  $T_w$  fluctuation decreased as the rotation was repeated. The longer cooling duration was considerable after 5 periods ( $t = 16.5 \text{ s}$ ). The change in  $q_w$  indicated maximal value at the stagnation point. At earlier stage of the cooling, change in  $q_w$  at the stagnation point was very sharp but gradually approached to shape of plateau due to the increase in the liquid-solid contact time specified with the rotational speed and the characteristic length of  $W_s$ . The amplitude of fluctuation in  $q_w$  also decreased with time after  $t_{wet,i}$  and finally disappeared after  $t_{wet,f}$ . The features of  $T_w$  and  $q_w$  changes shown in Fig.7(b) exactly corresponded to the visual observation of spreading wetting front in the circumferential direction after  $t_{wet,i}$ .

### 3.5. Characteristics of boiling curve during laminar jet quenching

A typical boiling curve for the condition of  $N = 60 \text{ rpm}$ ,  $T_l = 20^\circ\text{C}$ ,  $T_{b0} = 776^\circ\text{C}$  and  $Q = 10 \text{ L/min}$  is shown in Fig.8. The locus of the boiling curve was depicted with the black dots which were retrieved at the interval of 2 ms from the inverse solution of  $q_w$  and  $T_w$  as shown in Fig.7(a). The red dots plotted in sync with the rotational period of 1 s, indicate the boiling curve at the stagnation point.

In Fig.8(a) the locus of the boiling iterated a counterclockwise loop in accordance with the cylinder rotation and the loop moved from the higher wall superheat region to the lower one as the cooling time elapsed. Noting change in the slope of the boiling curve denoted with the red dots, we can see the transient boiling heat transfer on the stagnation point is categorized into three regions: Single phase heat transfer (S.P.) region, Nucleate boiling (N.B.) region and Transition boiling (T.B.) region. The single phase and nucleate boiling heat transfers indicated positive slope but the transition boiling was characterized with negative slope. In the present experimental data, film boiling (F.B.) region could not be observed in boiling curves. Even though the boiling situation was in "Non-wetted regime (a)" given in Figs.6 and 7 (a), partial and intermittent liquid-solid contacts on the stagnation point were implied from the result of Fig.8(b). At earlier stage larger loop was drawn due to accordance with passing on the wet and dry areas, but after the single phase heat transfer region included fully wetted situation denoted with  $t_{wet,f}$ , the boiling curve indicated monotonic change.



ab

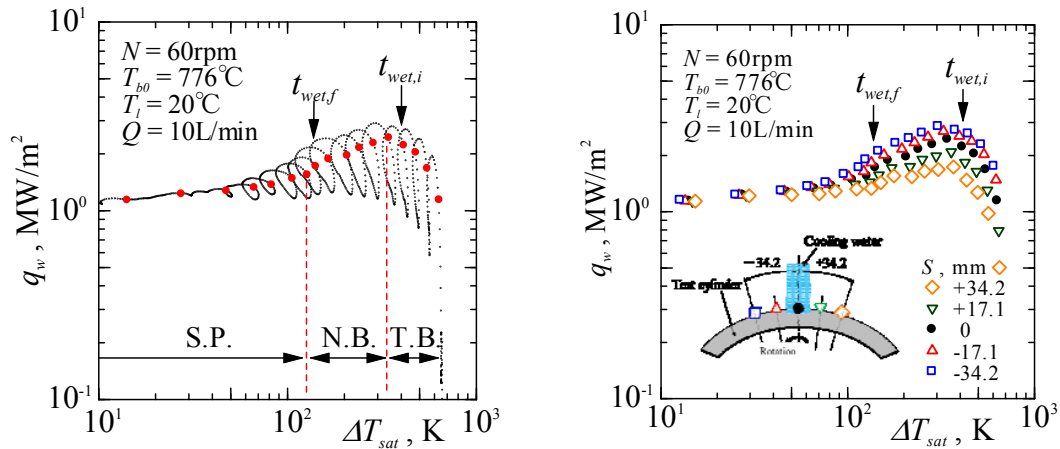


Fig.8 Boiling curve during rotating of cylinder. (a) locus of boiling curve (b) comparison of boiling curves at circumferential positions

Figure 8(b) shows the boiling curves at different circumference positions which were 17 mm and 34 mm ahead or behind the stagnation point. The maximum heat flux of each boiling curve increased as the circumference position changed from  $S = +34$  mm (behind the stagnation point) to  $S = -34$  mm (ahead the stagnation point).

Figure 9 shows the comparisons of the boiling curves evaluated at the stagnation point for different laminar flow rate, degree of liquid subcooling, respectively. For reference, the two correlations of single phase heat transfer coefficient in impinging jet cooling on the stagnation zone and film boiling heat transfer coefficient in subcooled jet impingement are given as Eqs.(1) and (2) by Liu, X. et al. [5] and Liu, Z.H. and Wang, J. [6]. These two correlations were derived by theoretical analysis for the stationary heated surface and steady state heat transfer.

In Fig.9(a) the boiling curves at  $Q = 6$  and  $10$  L/min indicate single phase convective heat transfer, nucleate boiling and transition boiling regions as denoted with S.P., N.B. and T.B.. It is found that the boiling curves in transient laminar jet cooling were similar with a pool boiling curve but the wall superheat at the maximum heat flux recorded about 300 K which is one digit higher than that of a typical pool boiling curve. The S.P. and N.B. regions are distinguished by change in the slope of the boiling curve, and the N.B. and T.B. regions are separated with the maximal heat flux point. The wall superheat recording the maximal heat flux was found to shift slightly to higher superheat side as increase in laminar flow rate. As the laminar flow rate  $Q$  increased beyond 10 L/min, nucleate boiling region appeared to vanish, and the boiling curves indicating positive slope approached to the similar relationships given by Eq.(1). In case of maximum laminar flow rate of 23 L/min, the transition boiling region was not observed and the heat flux of the measured boiling curve was about 25 % lower than Eq. (1). Film boiling region correlated with Eq.(2) was not appeared in the measured boiling curves. Much higher initial wall superheat would be needed to maintain the film boiling region.

In Fig.9(b), when the degree of subcooling  $\Delta T_{sub}$  increased beyond 80 K, the transition boiling region shrank, namely the maximal point was shifted to higher wall superheat region as  $\Delta T_{sub}$  increased. According to the boiling curve shift to high wall superheat regime,  $\Delta T_{sub}$  and  $Q$  have a similar effect. Under high  $\Delta T_{sub}$  and  $Q$  conditions, characteristic of the heat transfer below the wall superheat at the maximum heat flux point indicated very similar with the single phase convective heat transfer on the stagnation point. This fact also supported with the observation of the

$$Nu_{d,o} = \begin{cases} 0.715 Re_d^{1/2} Pr^{0.4} & 0.15 < Pr < 3 \\ 0.797 Re_d^{1/2} Pr^{1/3} & Pr > 3 \end{cases} \quad \text{Region 1: Stagnation zone } (r/d < 0.787) \quad (1)$$

$$\text{Nu} \left( \frac{q_w d_j}{\Delta T_{\text{sat}} \lambda_l} \right) \approx 2 \text{Re}_l^{1/2} \text{Pr}_l^{1/6} ((\lambda_v / \lambda_l) (\Delta T_{\text{sub}} / \Delta T_{\text{sat}}))^{1/2} \quad (2)$$

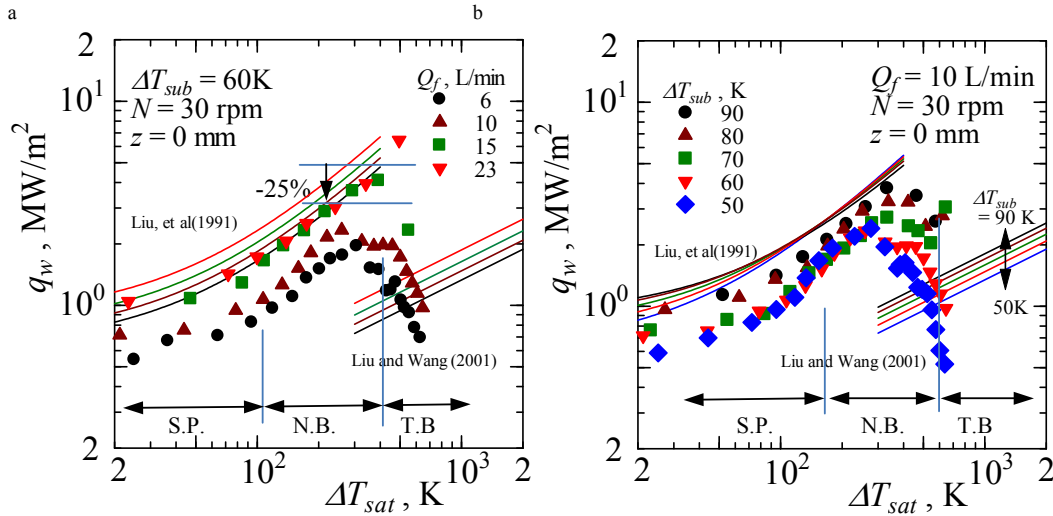


Fig.9 Comparison of boiling curves at the stagnation point; (a)effect of flow late, (b) effect of liquid subcooling

rewetting process shown in Figs.5 and 6.

#### 4. Conclusions

The experimental study on the subcooled laminar jet quenching on the rotating hot hollow cylinder which simulates quenching of hot strips on the ROT has been done for the extensive range of the flow rate, the jet temperature and the rotational speed. The highlights of the results are broadly concluded below.

1. The propagation of the wetting area during the laminar jet quenching on the rotating hollow cylinder depended strongly on the moving direction of the hot surface. And the characteristic of the wetting area propagation with time was categorized into the four regimes based on change in propagation of the wetting front in the circumferential direction.
2. The wetting temperature below which stable surface wetting situation could be seen on the stagnation area was very sensitive against the laminar jet temperature and the laminar flow rate.
3. The boiling curve on the stagnation area was divided into the boiling region being similar with a pool boiling curve but it shifted for much higher wall superheat region. As the liquid subcooling and the laminar flow rate increased, the single phase convective heat transfer region dominated on the boiling curve and it was comparable with the existing theoretical correlation on the stagnation area of the impinging jet for steady state and stationary heated surface.

#### Acknowledgements

The authors gratefully acknowledge the ISIJ (Iron and Steel Institute of Japan) for financial support of this study. Also Mr. Ryouta MAEMA, Mr. Shouta KANEGAE are gratefully acknowledged for their supports making the experimental apparatus and data processing.

## References

- [1] Gradeck, M., Kouachi, A., Lebouché, M., Volle, F., Maillet, D., Boreau, J.L., Boiling curves in relation to quenching of a high temperature moving surface with liquid jet impingement, *Int. J. Heat and Mass Transfer*, 52 (2009) 1094–1104
- [2] Aloke Kumar Mozumder, Mitsutake, Y. and Monde, M., Subcooled water jet quenching phenomena for a high temperature rotating cylinder, *Int. J. of Heat and Mass Transfer*, 68 (2014) 466–478.
- [3] Arima, H., Monde, M. and Mitsutake, Y., Estimation of Surface Temperature and Heat Flux using Inverse Solution for One Dimensional Heat Conduction, *Thermal Science and Engineering*, 10 (2002) 27–37.
- [4] Mitsutake, Y., Monde, M., Heat transfer during transient cooling of high temperature surface with an impinging jet, *Heat and Mass Transfer*, 37 (2001) 321–328.
- [5] Liu, X., Lienhard, J. S. and Lombard, J. S., “Convective Heat Transfer by Impingement of Circular Liquid Jets”, *Trans. ASME Heat Transfer*, 113 (1991) 571–582.
- [6] Liu, Z.H. and Wang, J., “Study on film boiling heat transfer for water jet impinging on high temperature flat plate”, *Int. J. Heat and Mass Transfer*, 40 (2001) 2475–2481.